



Cite this: *Dalton Trans.*, 2023, **52**, 5496

Received 9th February 2023,  
Accepted 28th March 2023

DOI: 10.1039/d3dt00425b

rs.c.li/dalton

## Substitution lability of the perfluorinated Cp\* ligand in Rh(i) complexes†

Joshua Parche, Susanne M. Rupf, Robin Sievers and Moritz Malischewski \*

Several cationic rhodium(i) complexes  $[\text{Rh}(\text{COD})\text{L}_2][\text{C}_5(\text{CF}_3)_5]^-$  have been synthesized through substitution of the weakly bound  $[\text{C}_5(\text{CF}_3)_5]^-$  ligand from  $[\text{Rh}(\text{COD})(\text{C}_5(\text{CF}_3)_5)]$ , further emphasizing its unique reactivity. Besides acetonitrile, pyridine derivatives with varying degrees of fluorination have been employed as ligands in order to investigate the influence of fluorination upon the binding affinity towards the resulting  $[\text{Rh}(\text{COD})]^+$  fragment and the limit as to which the  $[\text{C}_5(\text{CF}_3)_5]^-$  ligand can be displaced. Furthermore, the newly synthesized compounds represent rare examples of rhodium complexes containing fluorinated pyridines as ligands.

## Introduction

Fluorinated ligands, in particular F- or  $\text{CF}_3$ -substituted aromatics, have been gaining increasing attention in organometallic chemistry over the last years. The electron withdrawing effect of fluorine may lead to a decreased bonding strength of fluorinated ligands towards metal centers in comparison to their electron rich counterparts. For example,  $\eta^6$ -fluorobenzenes coordinated at rhodium(i) centers have been shown to have lower binding affinity with increasing degree of fluorination.<sup>1</sup> These comparably weak binding interactions can be of great advantage in catalysis, for systems proceeding *via* an inner-sphere mechanism that requires vacant coordination sites for substrate binding. Due to the high reactivity and inherent instability of coordinatively unsaturated transition metal complexes, their vacant sites can be masked by labile ligands, which stabilize the respective complex while being easily displaced and not interfering with the catalytic process.<sup>1,2</sup> Furthermore, the strong carbon–fluorine bond is relatively inert towards potential side-reactions such as oxidative addition, while also decreasing the probability of coordination through the electron-withdrawing group itself (*e.g.* cyano groups).<sup>3,4</sup> In this sense, Weller *et al.* have demonstrated the synthesis of catalytically active rhodium(i) complexes containing a  $\eta^6$ -monofluorobenzene ligand, prepared by using a simple one-pot procedure starting from  $[\text{Rh}(\text{COD})_2][\text{BAR}^{\text{F}}_4]$  (COD = cycloocta-1,5-diene,  $\text{Ar}^{\text{F}} = \text{C}_6\text{H}_3-(3,5-\text{CF}_3)_2$ ).<sup>5</sup> The

respective bench-stable complexes  $[\text{Rh}(\text{C}_6\text{H}_5\text{F})(\text{R}_2\text{PCH}_2\text{PR}'_2)][\text{BAR}^{\text{F}}_4]$  ( $\text{R}, \text{R}' = \text{tBu}$  or  $\text{Cy}$ ) have been proven as efficient precatalysts for various reactions, including intermolecular hydroacylations and dehydrogenative couplings of substituted amine–boranes.<sup>5–10</sup> In addition, similar rhodium(i) complexes containing weaker coordinating 1,2-difluorobenzene or 1,2,3-trifluorobenzene ligands allowed the isolation and structural characterization of previously inaccessible amine–borane  $\sigma$ -complexes, *via* displacement of the weakly coordinating ligands.<sup>11,12</sup> Interestingly, the further reduced coordinating ability of 1,2,3,4-tetra- and pentafluorobenzene led to the  $\pi$ -complexation of the weakly coordinating anion (WCA)  $[\text{BAR}^{\text{F}}_4]^-$  in solution, forming zwitterionic complexes  $[\text{Rh}(\text{R}_2\text{PCH}_2\text{PR}'_2)_2(\eta^6-(3,5-(\text{CF}_3)_2\text{C}_6\text{H}_3)\text{BAR}^{\text{F}}_3)]$  (Fig. 1, top).<sup>12</sup> In order to access these complexes containing highly fluorinated benzenes, the use of  $[\text{Al}(\text{OR}^{\text{F}})_4]^-$ , popularized by the group of Krossing, proved to be crucial to avoid displacement of the respective fluorobenzene.<sup>13,14</sup> Complexes containing highly fluorinated benzenes were shown to effectively catalyze the Tishchenko reaction of cyclohexanecarboxaldehyde ( $\text{C}_6\text{H}_{11}\text{CHO}$ ), while leading to shorter reaction times for

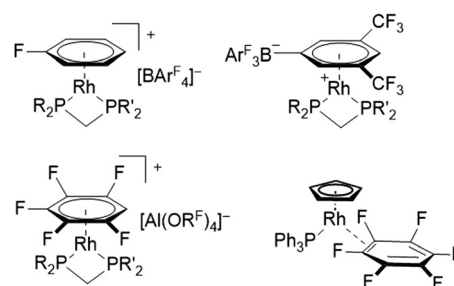


Fig. 1 Examples of rhodium(i) complexes with fluorinated aromatic ligands.

Freie Universität Berlin, Institute of Inorganic Chemistry, Fabeckstr. 34–36, 14195 Berlin, Germany. E-mail: moritz.malischewski@fu-berlin.de

† Electronic supplementary information (ESI) available: General conditions. Copies of NMR spectra. DFT calculations. CCDC 2240960 and 2240962. For ESI and crystallographic data in CIF or other electronic format see DOI: <https://doi.org/10.1039/d3dt00425b>



ligands with higher degrees of fluorination.<sup>14</sup> Although examples of  $\eta^6$ -coordination towards rhodium(I) centers have been described for fluorobenzenes carrying one to five fluorine substituents, no respective coordination compounds of hexafluorobenzene have been structurally characterized. Instead, a  $\eta^2$ -coordination was revealed after irradiation of rhodium alkene- or rhodium dihydride complexes in  $C_6F_6$ , leading to complexes with the general structure  $[Rh(C_5H_5)(PPh_3)(\eta^2-C_6F_6)]$  (Fig. 1, bottom).<sup>15–17</sup>

Thus, fluorinated benzenes were proved to be useful labile ligands which can mask reactive metal centers in order to facilitate catalytic reactions or to isolate reactive intermediates. In contrast, the use of weakly coordinated anionic aromatic ligands containing fluorine substituents is less explored.<sup>18</sup>

Undoubtedly the most prominent anionic aromatic ligand is the cyclopentadienyl ligand (Cp), which has gained enormous attention since its discovery in 1951, with known examples for nearly all metals.<sup>19,20</sup> Consequently numerous Cp derivatives with different steric and electronic properties have been synthesized and coordinated. Most Cp ligands however are electron rich, thus acting as strong  $\pi$ -donors, e.g. the permethylated Cp (Cp\*) being the best-known example. On the contrary, electron poor Cp derivatives are far less investigated, despite their potential to access electrophilic and oxidation resistant complexes with potential applications in catalysis.<sup>21–23</sup>

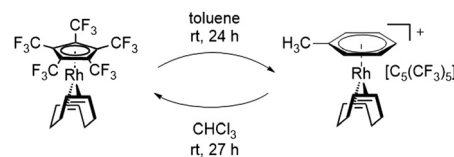
In this sense, an effective approach to access electron poor derivatives aims for perfunctionalization through the introduction of fluorine containing substituents. Nevertheless, perfluorinated Cp derivatives remain scarce due to their challenging synthesis and coordination.<sup>18</sup> For example, the fully fluorinated Cp,  $[C_5F_5]^-$ , has been first synthesized by Seppelt *et al.* in 1984. However, fast fluoride abstractions and further decomposition pathways prevented any coordination onto a metal center.<sup>24</sup> Its first coordination was achieved in 1992 by Hughes *et al.* through an in-coordination-sphere generation of the  $[C_5F_5]^-$  ligand by flash vacuum pyrolysis, forming the mixed ruthenocene  $[Ru(C_5(CH_3)_3)(C_5F_5)]$ .<sup>25</sup> In 2015, Sünkel *et al.* further showed the generation of the  $[C_5F_5]^-$  ligand by iterative deprotonations and electrophilic fluorinations of ferrocene (Fc), leading to  $[Fe(C_5H_5)(C_5F_5)]$ .<sup>26</sup> Interestingly, the corresponding diene  $HC_5F_5$  proved to be only slightly more acidic (estimated  $pK_a = 13–15$ ) than  $HC_5H_5$  ( $pK_a = 15.5$ ), due to the strong pronounced +M-effect of fluorine.<sup>24</sup> In contrast, the introduction of perfluorinated alkyl groups, such as  $CF_3$ , exhibit a stronger acidity, due to the absence of any conjugative donor effects. This effect is best visualized by the perfluorinated Cp\* analog,  $[C_5(CF_3)_5]^-$ , which was first reported by Lemal *et al.* in 1980 with a synthetically challenging approach starting from a perfluorinated dewarathiophene derivative.<sup>27</sup> In 1995, Chambers *et al.* simplified the synthetic access, by reacting hexachlorobuta-1,3-diene with KF, to obtain the non-isolatable  $K[C_5(CF_3)_5]$ , which was further reacted to form  $[NEt_4][C_5(CF_3)_5]$ .<sup>28</sup> In contrast to the  $HC_5H_5$  and  $HC_5F_5$ ,  $HC_5(CF_3)_5$  exhibits an extraordinary acidity ( $pK_a = -2.2$ ).<sup>27</sup> The remarkable electron deficiency observed in  $[C_5(CF_3)_5]^-$  and the

therefore expected weak bonding interactions to metal centers account for the difficulties concerning its coordination. Accordingly, more than four decades after its first synthesis the formation of metal complexes containing the  $[C_5(CF_3)_5]^-$  ligand remained elusive. In 2022 however, Malischewski *et al.* reported the first coordination of the perfluorinated Cp\* analog, through a salt metathesis reaction of  $[Rh(COD)Cl]_2$  with  $AgBF_4$  in presence of  $[NEt_4][C_5(CF_3)_5]$ , leading to the formation of the 18-electron complex  $[Rh(COD)(C_5(CF_3)_5)]$ .<sup>29</sup> While ordinary electron rich Cp ligands mostly show an irreversible binding to their respective metal centers and are only substituted by arenes or olefins in presence of other reagents, an exceptional reactivity was observed for the  $[C_5(CF_3)_5]^-$  ligand.<sup>30,31</sup> In presence of arenes and olefins,  $[C_5(CF_3)_5]^-$  was found to undergo an uncommon substitution, converting it into a WCA, further emphasizing the weak bonding interactions to the metal center. The displacement was shown by reacting  $[Rh(COD)(C_5(CF_3)_5)]$  with toluene, leading to the quantitative formation of the isolatable cationic arene complex  $[Rh(COD)(PhMe)][C_5(CF_3)_5]$ . Furthermore, the substitution of the Cp ligand was found to be fully reversible in weakly coordinating solvents such as  $CHCl_3$  or  $CH_2Cl_2$ , allowing it to switch between ligand and WCA depending on its environment (Scheme 1).<sup>29</sup>

In this work we further describe the investigation of the substitution lability of  $[C_5(CF_3)_5]^-$ . In this context, several donor ligands, but especially fluorinated pyridines were applied in order to tune the basicity of the potential ligands and to explore the limits at which the  $[C_5(CF_3)_5]^-$  ligand can be displaced (Fig. 2).

## Results and discussion

The  $[C_5(CF_3)_5]^-$  ligand was synthesized as its tetraethylammonium salt according to the procedure by Chambers *et al.* with addition of 18-crown-6 to increase the solubility of KF, and subsequently coordinated to the rhodium metal center according to the procedure by Malischewski *et al.*<sup>28,29,32</sup> The substitution reactions with the ligands shown in Fig. 2 could either be carried out in the respective ligand as solvent or in *n*-pentane with a moderate excess of the demanded ligand (except MeCN). When possible, it was preferred to perform the reaction in *n*-pentane as precipitation of the respective salts significantly reduced the reaction times. The reaction progress could be observed by <sup>19</sup>F NMR spectroscopy, through comparison of the coordinated  $[C_5(CF_3)_5]^-$  and anionic  $[C_5(CF_3)_5]^-$



**Scheme 1** Quantitative substitution of  $[C_5(CF_3)_5]^-$  in  $[Rh(COD)(C_5(CF_3)_5)]$  by toluene and fully reversible reaction in  $CHCl_3$ .



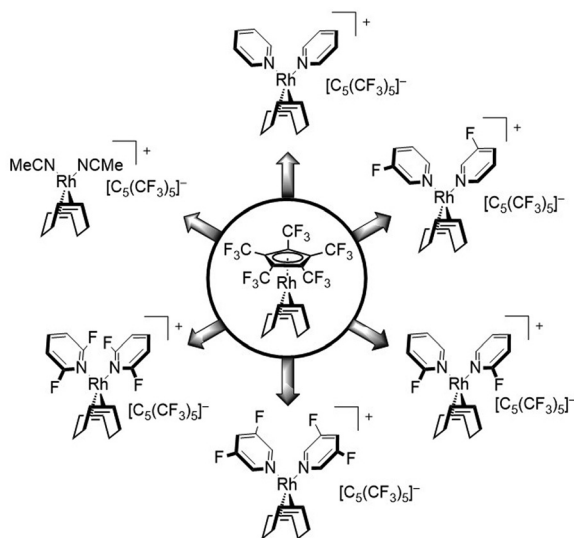


Fig. 2 Investigated substitutions of  $[C_5(CF_3)_5]^-$  in  $[Rh(COD)(C_5(CF_3)_5)]$  with different ligands.

signals, in analogy to the substitution by toluene.<sup>29</sup> The coordinated  $[C_5(CF_3)_5]^-$  ligand shows a singlet at  $\delta = -51.1$  ppm in  $CDCl_3$  (or  $\delta = -51.46$  ppm in  $CD_2Cl_2$ ), while the uncoordinated  $[C_5(CF_3)_5]^-$  possesses a downfield shifted signal at  $\delta = -50.18$  ppm in  $CDCl_3$  (or  $\delta = -50.52$  ppm in  $CD_2Cl_2$ ). Integration of the respective signals allows to observe the ratio of coordinated to non-coordinated  $[C_5(CF_3)_5]^-$ . Any unreacted  $[Rh(COD)(C_5(CF_3)_5)]$  can be removed from cationic complexes by washing the respective mixture with *n*-pentane.

First, the substitution of the perfluorinated Cp\* from  $[Rh(COD)(C_5(CF_3)_5)]$  in MeCN was investigated, in order to assess the displacement of  $[C_5(CF_3)_5]^-$  by two N-donor ligands. It was found that stirring the reaction for 1 h at room temperature, led to the complete substitution of the Cp ligand, turning it into a WCA and quantitatively forming the isolatable cationic 16-electron complex  $[Rh(COD)(MeCN)_2][C_5(CF_3)_5]$  (Fig. 3). The  $^{19}F$  NMR spectrum revealed a singlet at  $\delta = -51.1$  ppm in  $CDCl_3$ , which is in agreement with the signals of  $[Rh(COD)$

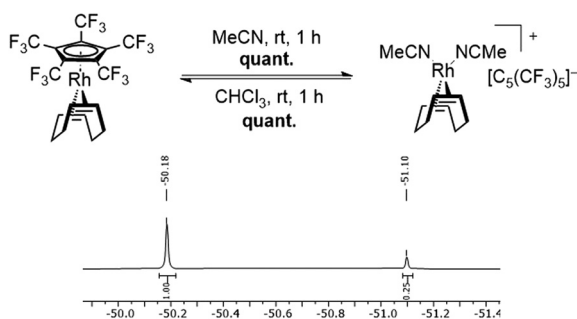


Fig. 3 Substitution of  $[C_5(CF_3)_5]^-$  in  $[Rh(COD)(C_5(CF_3)_5)]$  by MeCN and backreaction in  $CHCl_3$ .  $^{19}F$  NMR spectrum (377 MHz,  $CDCl_3$ , rt) measured 30 min after dissolving  $[Rh(COD)(MeCN)_2][C_5(CF_3)_5]$  in  $CDCl_3$ , showing the presence of both MeCN substituted complex (left) and  $[Rh(COD)(C_5(CF_3)_5)]$  (right).

$(PhMe)][C_5(CF_3)_5]$ .<sup>29</sup> In addition, a downfield shifted singlet was observed in the  $^1H$  NMR spectrum for the MeCN ligands ( $\delta = 2.20$  ppm in  $CD_2Cl_2$ ) in comparison to free MeCN ( $\delta = 1.97$  ppm in  $CD_2Cl_2$ ). Integration of the MeCN signals revealed a twofold coordination, when referencing to the COD signals.

Furthermore, it was found that the backreaction to  $[Rh(COD)(C_5(CF_3)_5)]$  proceeds rapidly, in comparison to the back reaction of  $[Rh(COD)(PhMe)][C_5(CF_3)_5]$ . Within 30 min after dissolving  $[Rh(COD)(MeCN)_2][C_5(CF_3)_5]$  in  $CDCl_3$  (15 mg  $mL^{-1}$ ), both signals of substituted as well as coordinated  $[C_5(CF_3)_5]^-$  are observed with a ratio of 4:1 respectively (Fig. 3). The equilibrium of the backreaction is strongly dependent on the concentration and is reached within 1 h. For a concentration of 2 mg  $mL^{-1}$  of  $[Rh(COD)(MeCN)_2][C_5(CF_3)_5]$  in  $CDCl_3$ , an equilibrium of cationic to neutral complex of 1:2, respectively, is observed. Under strongly diluted conditions (0.5 mg  $mL^{-1}$ )  $[Rh(COD)(MeCN)_2][C_5(CF_3)_5]$  can be fully reacted to  $[Rh(COD)(C_5(CF_3)_5)]$ . Dissolving the substituted complex in an increasingly polar solvent like  $CD_2Cl_2$  led to a significantly less pronounced backreaction, reaching an equilibrium of 10:1 of cationic to neutral complex at a comparable concentration as in Fig. 3 (15 mg  $mL^{-1}$ ).

Single crystals of  $[Rh(COD)(MeCN)_2][C_5(CF_3)_5]$  in the monoclinic  $P2_1/n$  space group were obtained from solvent mixtures of  $CH_2Cl_2$  and *n*-pentane by slowly cooling to  $-75$  °C (Fig. 4). The crystal structure revealed an averaged Rh–N bond length of 2.057(7) Å and an average Rh–C distance to the COD ligand of 2.121(7) Å, comparable to the bond lengths of  $[Rh(COD)(MeCN)_2][BF_4]$ , with average distances of 2.080(9) Å and 2.125(11) Å respectively.<sup>33</sup>

The substitution of  $[C_5(CF_3)_5]^-$  was further carried out with pyridine and several fluorine substituted derivatives (Scheme 2). Hereby, pyridine derivatives were employed with further decreasing basicity, depending on the position of the fluorine substituent as well as the degree of fluorination, in order to discover the substitution limit of  $[C_5(CF_3)_5]^-$ . The reactions could be performed by addition of the respective pyridine into a solution of  $[Rh(COD)(C_5(CF_3)_5)]$  in *n*-pentane, which led to a rapid precipitation of a colorless solid. For all substitutions shown in Scheme 2 (except 2,6-difluoropyridine),

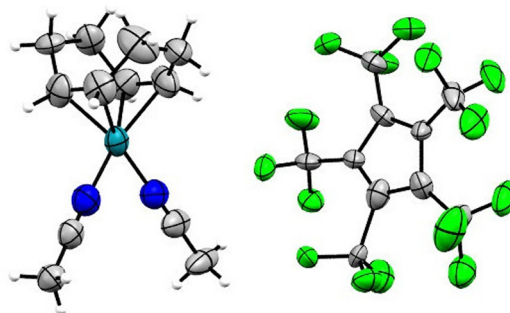
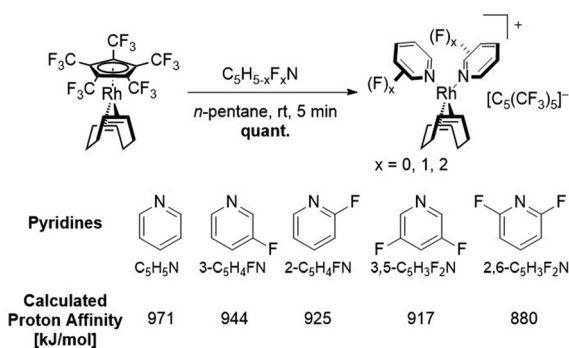


Fig. 4 Molecular structure in solid state of  $[Rh(COD)(MeCN)_2][C_5(CF_3)_5]$ . Disorders are omitted for clarity. Ellipsoids are depicted with 50% probability level. Color code: white-hydrogen; grey-carbon; blue-nitrogen; green-fluorine; light-blue-rhodium.





**Scheme 2** Substitution of  $[\text{C}_5(\text{CF}_3)_5]^-$  in  $[\text{Rh}(\text{COD})(\text{C}_5(\text{CF}_3)_5)]$  by different (fluorinated) pyridines with their corresponding proton affinities (B3LYP-D3/def2tzvp). The substitution by 2,6-difluoropyridine was carried out overnight.

$^1\text{H}$  NMR studies revealed a twofold coordination of the respective pyridine ligand, similar to the substitution with MeCN. However, no noteworthy shift of the pyridine signals was observed.  $^{19}\text{F}$  NMR spectra clearly confirmed the conversion of  $[\text{C}_5(\text{CF}_3)_5]^-$  into a WCA and furthermore showed a downfield shifted signal for the respective fluorine substituent(s), e.g.  $\delta = -68.3$  ppm for uncoordinated 2-fluoropyridine vs.  $\delta = -61.2$  ppm for 2-fluoropyridine coordinated complex  $[\text{Rh}(\text{COD})(2\text{-C}_5\text{H}_4\text{FN})_2][\text{C}_5(\text{CF}_3)_5]$ , in  $\text{CD}_2\text{Cl}_2$ .

Single crystals of  $[\text{Rh}(\text{COD})(3\text{-C}_5\text{H}_4\text{FN})_2][\text{C}_5(\text{CF}_3)_5]$  were obtained from solvent mixtures of  $\text{CH}_2\text{Cl}_2$  and *n*-pentane by slowly cooling to  $-75$  °C. The compound crystallizes in the triclinic space group  $P\bar{1}$ . The asymmetric unit contains two  $[\text{Rh}(\text{COD})(3\text{-C}_5\text{H}_4\text{FN})_2][\text{C}_5(\text{CF}_3)_5]$  fragments, further confirming the twofold coordination of the pyridines (Fig. 5). Additionally, the solid-state structure shows an average Rh–N bond length of 2.111(3) Å and an average of 2.133(5) Å for the Rh–C distance to the COD ligand. A database survey in the Cambridge Crystallographic Database (CSD) revealed no results for rhodium complexes with fluorinated pyridine ligands, thus  $[\text{Rh}(\text{COD})(3\text{-C}_5\text{H}_4\text{FN})_2][\text{C}_5(\text{CF}_3)_5]$  represents a rare example thereof.

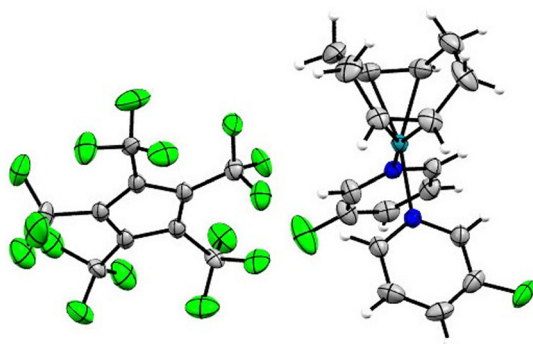


**Fig. 5** Molecular structure in solid state of  $[\text{Rh}(\text{COD})(3\text{-C}_5\text{H}_4\text{FN})_2][\text{C}_5(\text{CF}_3)_5]$ . Disorders are omitted for clarity. Ellipsoids are depicted with 50% probability level. Color code: white-hydrogen; grey-carbon; blue-nitrogen; green-fluorine; light-blue-rhodium.

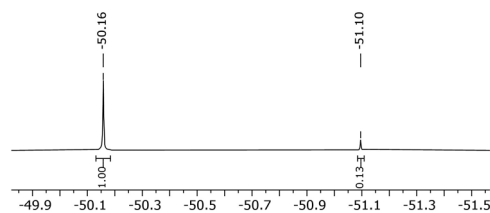


**Fig. 6**  $^{19}\text{F}$  NMR spectrum (377 MHz,  $\text{CDCl}_3$ , rt) of  $[\text{Rh}(\text{COD})(3\text{-C}_5\text{H}_4\text{FN})_2][\text{C}_5(\text{CF}_3)_5]$  after 3 d in  $\text{CDCl}_3$  at rt.

Surprisingly in contrast to the MeCN and toluene substitutions, no backreaction was observed for the pyridine substituted complexes in solution with  $\text{CD}_2\text{Cl}_2$ , except for the 2,6-difluoropyridine substituted complex. When dissolving  $[\text{Rh}(\text{COD})(\text{C}_5\text{H}_5\text{N})_2][\text{C}_5(\text{CF}_3)_5]$  in  $\text{CHCl}_3$ , no backreaction was observed either, despite prolonged reaction times (up to 4 d). Dissolving  $[\text{Rh}(\text{COD})(3\text{-C}_5\text{H}_4\text{FN})_2][\text{C}_5(\text{CF}_3)_5]$  in coordinating solvents such as MeCN did not lead to a substitution of the pyridine ligands, which was confirmed by  $^1\text{H}$  NMR. The backreaction of  $[\text{Rh}(\text{COD})(3\text{-C}_5\text{H}_4\text{FN})_2][\text{C}_5(\text{CF}_3)_5]$  to  $[\text{Rh}(\text{COD})(\text{C}_5(\text{CF}_3)_5)]$  proved to be minimal in  $\text{CHCl}_3$ , despite low concentrations and prolonged reaction times (Fig. 6). On the other hand, substitution of complexes  $[\text{Rh}(\text{COD})(2\text{-C}_5\text{H}_4\text{FN})_2][\text{C}_5(\text{CF}_3)_5]$  and  $[\text{Rh}(\text{COD})(3,5\text{-C}_5\text{H}_3\text{F}_2\text{N})_2][\text{C}_5(\text{CF}_3)_5]$  showed to be reversible in  $\text{CDCl}_3$ , so they could be fully converted back into  $[\text{Rh}(\text{COD})(\text{C}_5(\text{CF}_3)_5)]$ .

In strong contrast, the substitution with 2,6-difluoropyridine behaved differently in comparison to the other conducted pyridine substitutions. Performing the reaction in *n*-pentane did not lead to a fast precipitation of a solid, instead a yellow emulsion was formed after stirring the reaction overnight, discoloring the yellow *n*-pentane solution. After removing the remaining solvent the residue was washed with *n*-pentane, revealing an insoluble solid, strongly indicating the formation of a cationic complex under the given conditions. While  $^1\text{H}$  NMR spectra revealed the presence of two equivalents of 2,6-difluoropyridine when referenced to the COD signals, no signals of substituted  $[\text{C}_5(\text{CF}_3)_5]^-$  could be observed in the  $^{19}\text{F}$  NMR spectrum in either  $\text{CD}_2\text{Cl}_2$  or  $\text{CDCl}_3$ , indicating a rapid backreaction to  $[\text{Rh}(\text{COD})(\text{C}_5(\text{CF}_3)_5)]$  (see ESI, Fig. 20 and 21†). Elemental analysis studies however strongly indicate that the substitution with 2,6-difluoropyridine did proceed, as well as IR spectra of the newly formed species, which show new bands with strong similarities compared to IR spectra of the other (fluoro)pyridine substituted complexes (see Experimental section). It is therefore likely, that 2,6-difluoropyridine is able to substitute  $[\text{C}_5(\text{CF}_3)_5]^-$ , however the resulting complex  $[\text{Rh}(\text{COD})(2,6\text{-C}_5\text{H}_3\text{F}_2\text{N})_2][\text{C}_5(\text{CF}_3)_5]$  is rather unstable, due to the backreaction to  $[\text{Rh}(\text{COD})(\text{C}_5(\text{CF}_3)_5)]$  in solution.

## Conclusion

In conclusion, substitution of the  $[\text{C}_5(\text{CF}_3)_5]^-$  ligand of  $[\text{Rh}(\text{COD})(\text{C}_5(\text{CF}_3)_5)]$  was investigated with different N-donor



ligands, emphasizing its extraordinary electron deficiency and the weak bonding interactions towards the metal center. Hereby the displacement of the  $[C_5(CF_3)_5]^-$  ligand was first investigated with MeCN, leading to the formation of isolatable 16-electron complex  $[Rh(COD)(MeCN)_2][C_5(CF_3)_5]$ . Different pyridines with decreasing basicities were subsequently employed, to explore the limits of the substitution for the  $[C_5(CF_3)_5]^-$  ligand. While all pyridines were shown to quantitatively substitute the perfluorinated Cp\* ligand, the stability of the resulting cationic complexes was found to be strongly dependent on the basicity of the competing ligand. Cationic complexes containing relatively basic ligands, such as unsubstituted pyridine, were found to be stable in weakly coordinating solvents (e.g.,  $CHCl_3$  or  $CH_2Cl_2$ ), whereas for pyridines with weaker basicities, e.g. 2,6-difluoropyridine, the substitution proved to be fully reversible in solution, favouring the reformation of  $[Rh(COD)(C_5(CF_3)_5)]$ . In general, the ionic products are less stable in  $CHCl_3$  than in  $CH_2Cl_2$ . Furthermore, newly synthesized complexes  $[Rh(COD)(C_5H_{5-x}F_xN)_2][C_5(CF_3)_5]$  represent rare examples of rhodium(i) complexes containing (fluorinated) pyridine ligands.

## Experimental

### General procedure

The substitutions with different pyridine derivatives were carried out by dissolving  $[Rh(COD)(C_5(CF_3)_5)]$  (15.0 mg, 24.0  $\mu$ mol, 1.0 eq.) with anhydrous *n*-pentane (1 mL) in a 10 mL Schlenk tube, followed by addition of the respective pyridine (0.2 mL, excess). The solution was then stirred at rt for 5 min, after which a colorless precipitate formed. The solvent was removed under high vacuum and the residue was washed with *n*-pentane ( $2 \times 1$  mL). The remaining solvent was removed under high vacuum to afford the respective cationic complex.

### Synthetic procedures

**Preparation of  $[Rh(COD)(MeCN)_2][C_5(CF_3)_5]$ .**  $[Rh(COD)(C_5(CF_3)_5)]$  (15.0 mg, 24.0  $\mu$ mol, 1.0 eq.) was placed in a 10 mL Schlenk tube and dissolved in anhydrous MeCN (2 mL, excess). The solution was stirred at rt for 1 h and the solvent was removed under high vacuum. The residue was washed with *n*-pentane ( $2 \times 1$  mL) and the remaining solvent was removed under high vacuum, to afford  $[Rh(COD)(MeCN)_2][C_5(CF_3)_5]$  (16.8 mg, 24.0  $\mu$ mol, quant.) as a yellow solid.

**$^1H$  NMR** (600 MHz,  $CD_2Cl_2$ )  $\delta$  [ppm]: 4.43 (s, 4H), 2.45 (m, 4H), 2.20 (s, 6H), 1.94 (q,  $^3J = 8.1$  Hz, 4H).  **$^{13}C\{^1H\}$  NMR** (151 MHz,  $CD_2Cl_2$ )  $\delta$  [ppm]: 125.1 (s), 123.3 (s), 122.2 (s), 85.8 (d,  $^1J_{Rh} = 12.5$  Hz), 30.9 (s).  **$^{19}F$  NMR** (377 MHz,  $CD_2Cl_2$ )  $\delta$  [ppm]: -50.5 (s, 15F). **FT-IR** (ATR)  $\nu$  [ $cm^{-1}$ ]: 2963 (w), 2322 (w), 2293 (w), 1648 (w), 1497 (m), 1205 (s), 1108 (s), 972 (m), 875 (w), 802 (m), 633 (m). **HRMS** (ESI-TOF, positive)  $m/z$  for  $[C_{10}H_{15}NRh]^+$  calculated: 252.0260; measured: 252.0260. **HRMS** (ESI-TOF, negative)  $m/z$  for  $[C_{10}F_{15}]^-$  calculated: 404.9766; measured: 404.9486. **EA** ( $C_{22}H_{18}F_{15}N_2Rh$ ) calculated:

C: 37.84%, H: 2.60%, N: 4.01%; measured: C: 37.86%, H: 2.60%, N: 4.02%.

**Preparation of  $[Rh(COD)(C_5H_5N)_2][C_5(CF_3)_5]$ .** The substitution was performed according to the general procedure with anhydrous pyridine, to afford  $[Rh(COD)(C_5H_5N)_2][C_5(CF_3)_5]$  (18.6 mg, 24.0  $\mu$ mol, quant.) as a pale-yellow solid.

**$^1H$  NMR** (600 MHz,  $CD_2Cl_2$ )  $\delta$  [ppm]: 8.62–8.56 (m, 4H), 7.74 (tt,  $^3J = 7.7$  Hz,  $^4J = 1.6$  Hz, 2H), 7.37–7.31 (m, 4H), 4.09 (s, 4H), 2.67–2.57 (m, 4H), 2.04 (q,  $^3J = 7.9$  Hz, 4H).  **$^{13}C\{^1H\}$  NMR** (151 MHz,  $CD_2Cl_2$ )  $\delta$  [ppm]: 149.9 (s), 138.9 (s), 126.2 (s), 124.7 (s), 122.9 (s), 85.7 (d,  $^1J_{Rh} = 12.1$  Hz), 30.5 (s).  **$^{19}F$  NMR** (565 MHz,  $CD_2Cl_2$ )  $\delta$  [ppm]: -50.5 (s, 15F). **FT-IR** (ATR)  $\nu$  [ $cm^{-1}$ ]: 3021 (w), 2965 (w), 2925 (w), 2894 (w), 2877 (w), 2844 (w), 2360 (w), 1600 (w), 1496 (m), 1444 (m), 1296 (w), 1201 (vs), 1111 (vs), 997 (m), 971 (m), 874 (w), 836 (w), 802 (w), 760 (s), 698 (s), 632 (s). **HRMS** (ESI-TOF, negative)  $m/z$  for  $[C_{10}F_{15}]^-$  calculated: 404.9766; measured: 404.9686. **EA** ( $C_{28}H_{22}F_{15}N_2Rh$ ) calculated: C: 43.43%, H: 2.86%, N: 3.62%; measured: C: 44.60%, H: 3.13%, N: 3.57%.

**Preparation of  $[Rh(COD)(3-C_5H_4FN)_2][C_5(CF_3)_5]$ .** The substitution was performed according to the general procedure with anhydrous 3-fluoropyridine, to afford  $[Rh(COD)(3-C_5H_4FN)_2][C_5(CF_3)_5]$  (19.5 mg, 24.0  $\mu$ mol, quant.) as a yellow solid.

**$^1H$  NMR** (600 MHz,  $CD_2Cl_2$ )  $\delta$  [ppm]: 8.54 (t,  $^3J = 2.5$  Hz, 2H), 8.46 (dd,  $^3J = 5.4$  Hz, 2H), 7.57–7.51 (m, 2H), 7.39 (dt,  $^3J = 8.6$ ,  $^3J = 5.3$  Hz, 2H), 4.12 (s, 4H), 2.68–2.59 (m, 4H), 2.06 (q,  $^3J = 7.7$  Hz, 4H).  **$^{13}C\{^1H\}$  NMR** (151 MHz,  $CD_2Cl_2$ )  $\delta$  [ppm]: 161.2 (s), 159.5 (s), 146.7 (d,  $J = 4.4$  Hz), 139.3 (d,  $J = 29.6$  Hz), 127.7 (d,  $J = 6.2$  Hz), 126.8 (d,  $J = 17.5$  Hz), 86.9 (d,  $^1J_{Rh} = 12.0$  Hz), 30.9 (s).  **$^{19}F$  NMR** (565 MHz,  $CD_2Cl_2$ )  $\delta$  [ppm]: -50.5 (s, 15F), -119.4 (s, 2F). **FT-IR** (ATR)  $\nu$  [ $cm^{-1}$ ]: 3011 (w), 2957 (w), 2894 (w), 2847 (w), 1586 (w), 1481 (m), 1435 (m), 1258 (m), 1208 (vs), 1117 (vs), 976 (w), 845 (m), 799 (s), 696 (s), 633 (s), 537 (m). **HRMS** (ESI-TOF, negative)  $m/z$  for  $[C_{10}F_{15}]^-$  calculated: 404.9766; measured: 404.9486. **EA** ( $C_{28}H_{20}F_{17}N_2Rh$ ) calculated: C: 41.50%, H: 2.49%, N: 3.46%; measured: C: 41.88%, H: 2.71%, N: 3.59%.

**Preparation of  $[Rh(COD)(2-C_5H_4FN)_2][C_5(CF_3)_5]$ .** The substitution was performed according to the general procedure with anhydrous 2-fluoropyridine, to afford  $[Rh(COD)(2-C_5H_4FN)_2][C_5(CF_3)_5]$  (19.5 mg, 24.0  $\mu$ mol, quant.) as an orange solid.

**$^1H$  NMR** (600 MHz,  $CD_2Cl_2$ )  $\delta$  [ppm]: 8.49 (s, 2H), 7.85 (q,  $^3J = 7.6$  Hz, 2H), 7.29 (s, 2H), 7.06–6.98 (d,  $^3J = 8.3$  Hz, 2H), 4.19 (s, 4H), 2.69–2.60 (m, 4H), 2.02 (q,  $^3J = 7.8$  Hz, 4H).  **$^{13}C\{^1H\}$  NMR** (151 MHz,  $CD_2Cl_2$ )  $\delta$  [ppm]: 148.3 (d,  $J = 6.5$  Hz), 144.4 (s), 125.0 (s), 123.7 (s), 123.2 (s), 112.4 (s), 85.1 (d,  $^1J_{Rh} = 12.5$  Hz), 30.9 (s).  **$^{19}F$  NMR** (565 MHz,  $CD_2Cl_2$ )  $\delta$  [ppm]: -50.5 (s, 15F), -61.2 (s, 2F). **FT-IR** (ATR)  $\nu$  [ $cm^{-1}$ ]: 3012 (w), 2962 (w), 2922 (w), 2894 (w), 2845 (w), 1615 (m), 1576 (w), 1533 (m), 1479 (s), 1446 (s), 1337 (m), 1260 (m), 1205 (vs), 1100 (vs), 865 (s), 800 (s), 771 (vs), 734 (m), 696 (m), 633 (vs), 560 (m). **HRMS** (ESI-TOF, negative)  $m/z$  for  $[C_{10}F_{15}]^-$  calculated: 404.9766; measured: 404.9668. **EA** ( $C_{28}H_{20}F_{17}N_2Rh$ ) calculated: C:



41.50%, H: 2.49%, N: 3.46%; measured: C: 41.78%, H: 2.93%, N: 3.54%.

**Preparation of [Rh(COD)(3,5-C<sub>5</sub>H<sub>3</sub>F<sub>2</sub>N)<sub>2</sub>][C<sub>5</sub>(CF<sub>3</sub>)<sub>5</sub>].** The substitution was performed according to the general procedure with anhydrous 3,5-difluoropyridine, to afford [Rh(COD)(3,5-C<sub>5</sub>H<sub>3</sub>F<sub>2</sub>N)<sub>2</sub>][C<sub>5</sub>(CF<sub>3</sub>)<sub>5</sub>] (20.3 mg, 24.0 μmol, quant.) as a pale-yellow solid.

**<sup>1</sup>H NMR** (600 MHz, CD<sub>2</sub>Cl<sub>2</sub>) δ [ppm]: 8.46 (d, <sup>3</sup>J = 2.3 Hz, 4H), 7.41 (tt, <sup>3</sup>J = 7.9 Hz, <sup>4</sup>J = 2.3 Hz, 2H), 4.13 (s, 4H), 2.68–2.60 (m, 4H), 2.06 (q, <sup>3</sup>J = 7.6 Hz, 4H). **<sup>13</sup>C{<sup>1</sup>H} NMR** (151 MHz, CD<sub>2</sub>Cl<sub>2</sub>) δ [ppm]: 161.3 (s), 136.0 (d, J = 27.3 Hz), 125.1 (s), 115.5 (s), 87.5 (s), 30.8 (s). **<sup>19</sup>F NMR** (565 MHz, CD<sub>2</sub>Cl<sub>2</sub>) δ [ppm]: −50.6 (s, 15F), −116.3 (s, 4F). **FT-IR** (ATR) ν [cm<sup>−1</sup>]: 3088 (w), 3013 (w), 2961 (w), 2925 (w), 2897 (w), 2361 (w), 1599 (m), 1494 (m), 1438 (m), 1317 (m), 1210 (vs), 1116 (vs), 977 (m), 871 (m), 801 (w), 688 (m), 633 (m), 533 (m). **HRMS** (ESI-TOF, negative) m/z for [C<sub>10</sub>F<sub>15</sub>]<sup>−</sup> calculated: 404.9766; measured: 404.9684. **EA** (C<sub>28</sub>H<sub>18</sub>F<sub>19</sub>N<sub>2</sub>Rh) calculated: C: 39.74%, H: 2.14%, N: 3.31%; measured: C: 37.68%, H: 3.15%, N: 3.44%.

**Preparation of [Rh(COD)(2,6-C<sub>5</sub>H<sub>3</sub>F<sub>2</sub>N)<sub>2</sub>][C<sub>5</sub>(CF<sub>3</sub>)<sub>5</sub>].** The substitution was performed according to the general procedure with anhydrous 2,6-difluoropyridine but with a prolonged reaction time of 17 h, to afford [Rh(COD)(2,6-C<sub>5</sub>H<sub>3</sub>F<sub>2</sub>N)<sub>2</sub>][C<sub>5</sub>(CF<sub>3</sub>)<sub>5</sub>] (20.3 mg, 24.0 μmol, quant.) as a yellow solid.

**FT-IR** (ATR) ν [cm<sup>−1</sup>]: 2961 (w), 2927 (w), 2893 (w), 2844 (w), 1629 (s), 1567 (w), 1529 (m), 1493 (s), 1467 (w), 1329 (w), 1207 (vs), 1112 (vs), 1007 (s), 876 (w), 792 (vs), 741 (m), 697 (w), 632 (s), 569 (m). **EA** (C<sub>28</sub>H<sub>18</sub>F<sub>19</sub>N<sub>2</sub>Rh) calculated: C: 39.74%, H: 2.14%, N: 3.31%; measured: C: 39.76%, H: 2.18%, N: 3.32%.

## Conflicts of interest

There are no conflicts to declare.

## Acknowledgements

Gefördert durch die Deutsche Forschungsgemeinschaft (DFG)—Projekt Nummer 387284271—SFB 1349. Computing time was made available by High-Performance Computing ZEDAT/FU Berlin. The authors acknowledge the assistance of the Core Facility BioSupraMol supported by the DFG. The authors acknowledge generous support by the Fonds of the Chemical Industry (Kekulé fellowship for Robin Sievers).

## References

- S. D. Pike, I. Pernik, R. Theron, J. S. McIndoe and A. S. Weller, *J. Organomet. Chem.*, 2015, **784**, 75–83.
- S. T. H. Willems, P. H. M. Budzelaar, N. N. P. Moonen, R. de Gelder, J. M. M. Smits and A. W. Gal, *Chem. – Eur. J.*, 2002, **8**, 1310–1320.
- V. V. Grushin and H. Alper, *Chem. Rev.*, 1994, **94**, 1047–1062.
- R. J. Less, T. C. Wilson, M. McPartlin, P. T. Wood and D. S. Wright, *Chem. Commun.*, 2011, **47**, 10007–10009.
- A. B. Chaplin, J. F. Hooper, A. S. Weller and M. C. Willis, *J. Am. Chem. Soc.*, 2012, **134**, 4885–4897.
- A. Prades, M. Fernández, S. D. Pike, M. C. Willis and A. S. Weller, *Angew. Chem., Int. Ed.*, 2015, **54**, 8520–8524.
- I. Pernik, J. F. Hooper, A. B. Chaplin, A. S. Weller and M. C. Willis, *ACS Catal.*, 2012, **2**, 2779–2786.
- T. M. Douglas, J. L. Nôtre, S. K. Brayshaw, C. G. Frost and A. S. Weller, *Chem. Commun.*, 2006, 3408–3410.
- R. Dallanegra, A. P. M. Robertson, A. B. Chaplin, I. Manners and A. S. Weller, *Chem. Commun.*, 2011, **47**, 3763–3765.
- J. F. Hooper, R. D. Young, I. Pernik, A. S. Weller and M. C. Willis, *Chem. Sci.*, 2013, **4**, 1568–1572.
- T. M. Douglas, A. B. Chaplin, A. S. Weller, X. Yang and M. B. Hall, *J. Am. Chem. Soc.*, 2009, **131**, 15440–15456.
- A. L. Colebatch, A. I. McKay, N. A. Beattie, S. A. Macgregor and A. S. Weller, *Eur. J. Inorg. Chem.*, 2017, **2017**, 4533–4540.
- I. Krossing, *Chem. – Eur. J.*, 2001, **7**, 490–502.
- A. I. McKay, J. Barwick-Silk, M. Savage, M. C. Willis and A. S. Weller, *Chem. – Eur. J.*, 2020, **26**, 2883–2889.
- S. T. Belt, S. B. Duckett, M. Helliwell and R. N. Perutz, *J. Chem. Soc., Chem. Commun.*, 1989, 928–930.
- C. L. Higgitt, A. H. Klahn, M. H. Moore, B. Oelckers, M. G. Partridge and R. N. Perutz, *J. Chem. Soc., Dalton Trans.*, 1997, 1269–1280.
- L. Lefort, T. W. Crane, M. D. Farwell, D. M. Baruch, J. A. Kaeuper, R. J. Lachicotte and W. D. Jones, *Organometallics*, 1998, **17**, 3889–3899.
- R. Sievers, J. Parche, N. G. Kub and M. Malischewski, *Synlett*, 2023, DOI: [10.1055/s-0042-1751426](https://doi.org/10.1055/s-0042-1751426).
- T. J. Kealy and P. L. Pauson, *Nature*, 1951, **168**, 1039–1040.
- C. Janiak and H. Schumann, in *Adv. Organomet. Chem.*, ed. F. G. A. Stone and R. West, Academic Press, 1991, vol. 33, pp. 291–393.
- D. W. Macomber, W. P. Hart and M. D. Rausch, in *Adv. Organomet. Chem.*, Academic Press, 1982, vol. 21, pp. 1–55.
- S. Lauk and A. Schäfer, *Eur. J. Inorg. Chem.*, 2021, **2021**, 5026–5036.
- F. Mazzotta, G. Zitzer, B. Speiser and D. Kunz, *Chem. – Eur. J.*, 2020, **26**, 16291–16305.
- G. Paprott and K. Seppelt, *J. Am. Chem. Soc.*, 1984, **106**, 4060–4061.
- O. J. Curnow and R. P. Hughes, *J. Am. Chem. Soc.*, 1992, **114**, 5895–5897.
- K. Sünkel, S. Weigand, A. Hoffmann, S. Blomeyer, C. G. Reuter, Y. V. Vishnevskiy and N. W. Mitzel, *J. Am. Chem. Soc.*, 2015, **137**, 126–129.
- E. D. Laganis and D. M. Lemal, *J. Am. Chem. Soc.*, 1980, **102**, 6633–6634.
- R. D. Chambers, S. J. Mullins, A. J. Roche and J. F. S. Vaughan, *J. Chem. Soc., Chem. Commun.*, 1995, 841–842.



- 29 R. Sievers, M. Sellin, S. M. Rupf, J. Parche and M. Malischewski, *Angew. Chem., Int. Ed.*, 2022, e202211147.
- 30 D. W. Slocum, T. R. Engelmann, R. L. Fellows, M. Moronski and S. Duraj, *J. Organomet. Chem.*, 1984, **260**, C21–C25.
- 31 S. G. Shore, W. L. Hsu, M. R. Churchill and C. Bueno, *J. Am. Chem. Soc.*, 1983, **105**, 655–656.
- 32 R. Alberto, personal communication.
- 33 S. O. Kang, V. M. Lynch, V. W. Day and E. V. Anslyn, *Organometallics*, 2011, **30**, 6233–6240.

